JOURNAL OF INTEGRAL EQUATIONS
AND APPLICATIONS
Volume 30, Number 2, Summer 2018

INVERSE SCATTERING FOR SHAPE AND IMPEDANCE REVISITED

RAINER KRESS AND WILLIAM RUNDELL

ABSTRACT. The inverse scattering problem under consideration is to reconstruct both the shape and the impedance function of an impenetrable two-dimensional obstacle from the far field pattern for scattering of time-harmonic acoustic or E-polarized electromagnetic plane waves. We propose an inverse algorithm that is based on a system of nonlinear boundary integral equations associated with a single-layer potential approach to solve the forward scattering problem. This extends the approach we suggested for an inverse boundary value problem for harmonic functions in **[8]** and is a counterpart of our earlier work on inverse scattering for shape and impedance in **[7]**. We present the mathematical foundation of the method and exhibit its feasibility by numerical examples.

1. Introduction. The general task of inverse obstacle scattering theory for time harmonic acoustic and electromagnetic waves is to retrieve information on the shape of a scattering object D and its physical properties as given by its boundary condition from a knowledge of the scattered field at infinity, i.e., the far field pattern. The so-called Leontovich or impedance boundary condition

$$\frac{\partial u}{\partial \nu} + ik\lambda u = 0 \quad \text{on } \partial D \tag{1.1}$$

for the total field u and its normal derivative contains physical information on the scatterer D by the impedance function λ. In general, it is applied to scattering problems for penetrable obstacles to model them approximately by scattering problems for impenetrable obstacles in order to reduce the cost of numerical computations.

2010 AMS *Mathematics subject classification.* Primary 35J05, 35J25, 45Q05.

Keywords and phrases. Inverse scattering, Helmholtz equation, boundary integral equations, regularized Newton iterations.

The second author was supported in part by the National Science Foundation, award No. DMS-1620138.

Received by the editors on January 25, 2017.

DOI:10.1216/JIE-2018-30-2-293

In order to formulate the impedance obstacle scattering problem that we want to consider, let D be a simply connected bounded domain in $\mathbb{R}^2$ with C^2 boundary ∂D, and denote by ν the unit normal vector to ∂D oriented towards the complement $\mathbb{R}^2 \setminus \overline{D}$. Then, the scattering problem is to find the total wave $u = u^i + u^s \in H^1_{\rm loc}(\mathbb{R}^2 \setminus \overline{D})$ satisfying the Helmholtz equation

$$\Delta u + k^2 u = 0 \quad \text{in } \mathbb{R}^2 \setminus \overline{D} \tag{1.2}$$

with positive wave number k and the impedance boundary condition (1.1), where $\lambda \in C(\partial D)$ is a complex valued function. The incident wave u^i is assumed to be a plane wave $u^i(x) = e^{ik\,x\cdot d}$ with a unit vector d describing the direction of propagation, but we can also allow other incident waves such as point sources. The scattered wave u^s must satisfy the Sommerfeld radiation condition

$$\lim_{r\to\infty} \sqrt{r}\left(\frac{\partial u^s}{\partial r} - iku^s\right) = 0, \quad r = |r|, \tag{1.3}$$

uniformly with respect to all directions. We note that the condition

$$\operatorname{Re}\lambda \geq 0 \tag{1.4}$$

ensures the uniqueness of a solution to (1.1)–(1.3) (see [**3,** Theorem 2.12]). Existence may be established by seeking the solution in the form of a combined single- and double-layer potential and imitating the proof of Theorem 3.12 in [**3**].

The Sommerfeld radiation condition is equivalent to the asymptotic behavior of an outgoing cylindrical wave of the form

$$u^s(x) = \frac{e^{ik\,|x|}}{\sqrt{|x|}}\left\{u_\infty(\widehat{x}) + O\left(\frac{1}{|x|}\right)\right\}, \quad |x| \to \infty, \tag{1.5}$$

uniformly for all directions $\widehat{x} = x/|x|$ where the function u_∞ defined on the unit circle $\mathbb{S}^1$ is known as the far field pattern of u^s. The full inverse impedance obstacle scattering problem now is to determine both the boundary ∂D and the impedance function λ from a knowledge of the far field pattern u_∞ on $\mathbb{S}^1$ for one or several incident plane waves.

About 15 years ago [**7**], we proposed a solution method for the full inverse impedance obstacle problem by regularized Newton type iterations for the solution operator $\mathcal{F} : (\partial D, \lambda) \mapsto u_\infty$ that maps the boundary ∂D and the impedance function λ onto the far field pattern

u_∞ of the solution to (1.1)–(1.3). In that paper, we demonstrated the feasibility of this method by numerical examples and proved a local uniqueness result, i.e., injectivity for the Fréchet derivative of $\mathcal{F}$.

The approach in **[7]** is based on the characterization of the Fréchet derivative of $\mathcal{F}$ via an exterior impedance boundary value problem due to Hettlich **[4]**. In particular, the derivative with respect to the boundary in the direction q is given by the far field pattern $v_{\infty,q}$ of the radiating solution v_q of the impedance boundary value problem in $\mathbb{R}^2 \setminus \overline{D}$ with boundary condition

$$(1.6)\quad \frac{\partial v_q}{\partial \nu} + ik\lambda v_q = k^2 q\cdot\nu\, u + \frac{d}{ds}\left(q\cdot\nu\,\frac{du}{ds}\right) - ik\lambda\, q\cdot\nu\left(\frac{\partial u}{\partial \nu} - \kappa u\right)$$

on ∂D, where s denotes arc length, κ is the curvature of ∂D and u is the solution to (1.1)–(1.3). With $\partial D_q := \{x + q(x) : x \in \partial D\}$, this differentiability result follows from the estimate

$$\|u_{\infty,\partial D_q} - u_{\infty,\partial D} - v_{\infty,q}\|_{L^2(\mathbb{S}^1)} \le c\,\|q\|_{C^2(\partial D)}$$

for some positive constant c and all sufficiently small C^2 vector fields q on ∂D, see **[4]**. Just as with the corresponding Newton iteration schemes for inverse obstacle scattering for boundary conditions of sound-soft type (that is, Dirichlet conditions) and sound-hard (that is, Neumann conditions), the performance suffers due to the computational cost of setting up the iteration matrix. This requires the incorporation of the boundary values in (1.6) for all q spanning the chosen approximation subspace.

As a remedy, about ten years ago **[8]** we initiated modified Newton type iterations with reduced computational costs for a related inverse problem for the Laplace equation which later was extended to a wide range of inverse obstacle scattering problems. Its basic idea is to start from a boundary integral equation approach for the solution of the forward scattering problem, either via a potential approach or the direct approach via Green's representation formulas, to derive a system of two nonlinear integral equations for the unknown boundary ∂D and a density function on the boundary as a sort of slip variable. The derivatives of the corresponding operator can now simply be written down explicitly in terms of boundary integral operators which then offers computational advantages. For an overview and survey on this idea, the reader is referred to **[3,** subsection 5.4] and **[5]**. Thus far in the literature this approach has been applied only to a related impedance boundary value problem in electrostatic imaging [**1, 2**] but not to the full inverse impedance obstacle scattering problem. The purpose of the current paper is to fill this gap.

We begin in Section 2 with a short view on uniqueness and then proceed in Section 3 with the presentation of our solution method. This is followed in Section 4 by consideration of the relation of our method to Newton iterations for the operator equation in terms of $\mathcal{F}$. Finally, in Section 5, we illustrate the method by a couple of numerical examples.

For further recent approaches to the simultaneous reconstruction of the shape and the impedance in inverse obstacle scattering, the reader is referred to [**9, 10, 11, 12, 13, 14, 15**].

2. Uniqueness. Concerning uniqueness, i.e., identifiability, it is known that both the shape of D and the impedance function λ are uniquely determined by the far field patterns for an infinite number of incident plane waves with distinct directions (see [**3,** Theorem 5.6]). It remains a challenging open problem to establish uniqueness for one or a finite number of incident plane waves.

Theorem 2.1. *A disc with constant impedance coefficient is uniquely determined by the far field pattern for one incident plane wave.*

Proof. Using polar coordinates, the Jacobi-Anger expansion (see [**3**]) reads:

$$e^{ik\,x\cdot d} = \sum_{n=-\infty}^{\infty} i^n\,J_n(kr)\,e^{in\theta}, \quad x \in \mathbb{R}^2, \tag{2.1}$$

where θ is the angle between x and d and $r := |x|$. From this, it can be seen that the scattered wave u^s for scattering from a disc of radius R centered at the origin has the form

$$u^s(x) = \sum_{n=-\infty}^{\infty} a_n\,i^n\,H_n^{(1)}(kr)\,e^{in\theta}, \quad r > R, \tag{2.2}$$

with the coefficients

$$a_n = \frac{J_n'(kR) + i\lambda_n J_n(kR)}{H_n^{(1)'}(kR) + i\lambda H_n^{(1)}(kR)}. \tag{2.3}$$

We note that the uniqueness for the forward scattering problem ensures that the denominator in (2.3) is different from zero. Using the asymptotics of the Bessel and Hankel functions J_n and $H_n^{(1)}$ for large n, uniform convergence can be established for the series (2.2) in compact subsets of $\mathbb{R}^2 \setminus \{0\}$. In particular, this implies that the scattered wave u^s has an extension as a solution to the Helmholtz equation across the boundary into the interior of the disc, with the exception of the center.

Now, assume that two discs D_1 and D_2 with centers z_1 and z_2 have the same far field pattern $u_{\infty,1} = u_{\infty,2}$ for the scattering of one incident plane wave. Then, by Rellich's lemma [**3**], the scattered waves coincide $u_1^s = u_2^s$ in $\mathbb{R}^2 \setminus (D_1 \cup D_2)$, and we can identify $u^s = u_1^s = u_2^s$ in $\mathbb{R}^2 \setminus (D_1 \cup D_2)$. Now, assume that $z_1 \neq z_2$. Then, u_1^s has an extension into $\mathbb{R}^2 \setminus \{z_1\}$ and u_2^s an extension into $\mathbb{R}^2 \setminus \{z_2\}$. Therefore, u^s can be extended from $\mathbb{R}^2 \setminus (D_1 \cup D_2)$ into all of $\mathbb{R}^2$, that is, u^s is an entire solution to the Helmholtz equation. Consequently, since u^s also satisfies the radiation condition, it must identically vanish $u^s = 0$ in all of $\mathbb{R}^2$. Therefore, the incident field $u^i(x) = e^{ik\,x\cdot d}$ must satisfy the impedance condition on D_1 with radius R_1. This implies $\cos\theta + \lambda = 0$ for all $\theta \in [0, 2\pi]$. However, this is a contradiction, and therefore, $z_1 = z_2$.

In order to show that D_1 and D_2 have the same radius and the same impedance coefficient, we observe that, by symmetry, or by inspection of the explicit solution (2.2), the far field pattern for scattering of plane waves from a disc with constant impedance coefficient depends only upon the angle between the observation direction and the incident direction. Hence, knowledge of the far field pattern for one incident direction implies knowledge of the far field pattern for all incident directions. Now, the statement follows from uniqueness for infinitely many incident plane waves as mentioned above. □

3. The iteration method. We now proceed by describing an iterative algorithm for approximately solving the full inverse impedance problem by extending the method proposed in [**8**] to this case. For this, we recall the fundamental solution of the Helmholtz equation

$$\Phi(x, y) = \frac{i}{4}\, H_0^{(1)}(k|x - y|), \quad x \neq y,$$

in $\mathbb{R}^2$, in terms of the Hankel function $H_0^{(1)}$ of the first kind of order zero. Furthermore, following [**3**], we introduce two classical boundary integral operators in scattering theory, given by the single-layer operator

$$(S\varphi)(x) := 2\int_{\partial D} \Phi(x,y)\varphi(y)\,ds(y), \quad x \in \partial D, \tag{3.1}$$

and the corresponding normal derivative operator

$$(K'\varphi)(x) := 2\int_{\partial D} \frac{\partial \Phi(x,y)}{\partial \nu(x)}\,\varphi(y)\,ds(y), \quad x \in \partial D. \tag{3.2}$$

We note that, for $\partial D \in C^2$, both S and K' are compact from $C(\partial D)$ into itself. Additionally, we introduce the far field operator $S_\infty : C(\partial D) \to L^2(\mathbb{S}^1)$ by

$$(S_\infty\varphi)(\widehat{x}) := \frac{e^{i\pi/4}}{\sqrt{8\pi k}} \int_{\partial D} e^{-ik\,\widehat{x}\cdot y}\varphi(y)\,ds(y), \quad \widehat{x} \in \mathbb{S}^1, \tag{3.3}$$

and observe that $S_\infty\varphi$ represents the far field pattern of the single-layer potential with density φ on ∂D and that S_∞ is a compact operator.

Now, we can state the next theorem as the basis of our algorithm.

Theorem 3.1. *For a given incident field u^i and a given far field pattern u_∞, assume that the boundary ∂D, the impedance function λ and the density φ satisfy the system*:

$$\varphi - K'\varphi - ik\lambda S\varphi = 2\frac{\partial u^i}{\partial \nu}\bigg|_{\partial D} + 2ik\lambda u^i|_{\partial D} \tag{3.4}$$

and

$$S_\infty\varphi = u_\infty. \tag{3.5}$$

Then, ∂D and λ solve the inverse impedance problem.

Proof. Under the assumption of the theorem, as a consequence of (3.5), the single-layer potential

$$u^s(x) := \int_{\partial D} \Phi(x,y)\varphi(y)\,ds(y), \quad x \in \mathbb{R}^2 \setminus \overline{D},$$

has far field pattern u_∞ and, in view of the jump relations, as a consequence of (3.4), the superposition $u = u^i + u^s$ satisfies the impedance boundary condition. $\square$

We note that, for a given λ, the boundary integral equation (3.4) is uniquely solvable, provided k^2 is not a Dirichlet eigenvalue for $-\Delta$ in D.

The ill-posedness of the inverse impedance problem is reflected through the ill-posedness of the second equation (3.5). Note that the system (3.4)–(3.5) is linear with respect to the density φ and the impedance λ and nonlinear with respect to the boundary ∂D. We solve it by simultaneous linearization with respect to all three unknowns and iteration, i.e., by Newton iterations that require regularization due to the ill-posedness.

At this point, we note that the approach by Serranho **[14]** cited at the end of the introduction is, in principle, also based on the system (3.4)–(3.5). However, it is set up differently: given an approximation for the shape and the impedance function, it solves the ill-posed linear equation (3.5) for the density φ, and then, keeping φ fixed, linearizes (3.4) to update the shape and the impedance.

However, before proceeding, we need to formulate the straightforward extension of Theorem 3.1 to the case of more than one incident wave since, in general, we cannot expect to retrieve the three unknowns ∂D, λ and φ from only two equations.

Corollary 3.2. *For $M \in \mathbb{N}$, given incident fields $u_1^i, \ldots, u_M^i$ and corresponding far field patterns $u_{\infty,1}, \ldots, u_{\infty,M}$, assume that the boundary ∂D, the impedance function λ and the densities $\varphi_1, \ldots, \varphi_m$ satisfy the system*

$$\varphi_m - K'\varphi_m - ik\lambda S\varphi_m = 2\frac{\partial u_m^i}{\partial \nu}\bigg|_{\partial D} + 2ik\lambda u_m^i|_{\partial D} \tag{3.6}$$

and

$$S_\infty \varphi_m = u_{\infty,m} \tag{3.7}$$

for $m = 1, \ldots, M$. Then, ∂D and λ solve the inverse impedance problem.

For the linearization of the boundary integral operators we assume that the boundary curve ∂D is given by a regular 2π periodic parameterization

$$\partial D = \{z(t) : 0 \le t \le 2\pi\}. \tag{3.8}$$

Then, emphasizing the dependence of the operators on the boundary curve, we introduce the parameterized single-layer operator

$$\widetilde{S} : L^2[0,2\pi] \times C^2[0,2\pi] \longrightarrow L^2[0,2\pi]$$

as the integral operator

$$\widetilde{S}(\psi, z)(t) := \int_0^{2\pi} L(t,\tau;z)\,\psi(\tau)\,d\tau, \quad t \in [0,2\pi],$$

with kernel

$$L(t,\tau;z) := \frac{i}{2}\,H_0^{(1)}(k|z(t)-z(\tau)|)$$

and the parameterized normal derivative operator

$$\widetilde{K}' : L^2[0,2\pi] \times C^2[0,2\pi] \longrightarrow L^2[0,2\pi]$$

as the integral operator

$$\widetilde{K}'(\psi, z)(t) := \int_0^{2\pi} M(t,\tau;z)\,\psi(\tau)\,d\tau, \quad t \in [0,2\pi],$$

with kernel

$$M(t,\tau;z) := \frac{ik}{2}\,\frac{[z'(t)]^\perp \cdot [z(\tau)-z(t)]}{|z(t)-z(\tau)|}\,H_1^{(1)}(k|z(t)-z(\tau)|).$$

Here, we made use of ${H_0^{(1)}}' = -H_1^{(1)}$ with the Hankel function $H_1^{(1)}$ of order one and of the first kind. Furthermore, we denote $a^\perp := (a_2, -a_1)$ for any vector $a = (a_1, a_2)$, that is, $a^\perp$ is obtained by rotating a clockwise by 90 degrees. We also require the parameterized far field operator

$$\widetilde{S}_\infty : L^2[0,2\pi] \times C^2[0,2\pi] \longrightarrow L^2(\mathbb{S}^1),$$

given by

$$\widetilde{S}_\infty(\psi, z)(\widehat{x}) := \frac{e^{i\pi/4}}{\sqrt{8\pi k}} \int_0^{2\pi} e^{-ik\,\widehat{x}\cdot z(\tau)}\psi(\tau)\,d\tau, \quad \widehat{x} \in \mathbb{S}^1. \tag{3.9}$$

It follows that the parameterized form of the system (3.4)–(3.5) is given by

$$\psi - \widetilde{K}'(\psi, z) - ik\mu\widetilde{S}(\psi, z) = g(z, \mu) \tag{3.10}$$

and

$$\widetilde{S}_\infty(\psi, z) = u_\infty, \tag{3.11}$$

where we set

$$\psi := |z'|\,\varphi\circ z \quad \text{and} \quad \mu := |z'|\,\lambda\circ z \tag{3.12}$$

and

$$g(z,\mu) := 2[z']^\perp \cdot \mathrm{grad} u^i \circ z + 2ik\mu u^i \circ z. \tag{3.13}$$

This system needs to be solved for ψ, μ and z. We accomplish this via linearization. Given an approximation for (ψ, μ, z), we solve the linearized equations

$$\begin{aligned} &\eta - \widetilde{K}'(\eta, z) - ik\mu\widetilde{S}(\eta, z) - ik\gamma\widetilde{S}(\psi, z) - 2ik\gamma u^i \circ z \\ &-d\widetilde{K}'(\psi, z;\zeta) - ik\mu d\widetilde{S}(\psi, z;\zeta) - \partial_z g(z,\mu;\zeta) \\ &\qquad = g(z) - \psi + \widetilde{K}'(\psi, z) + ik\mu\widetilde{S}(\psi, z) \end{aligned} \tag{3.14}$$

and

$$\widetilde{S}_\infty(\eta, z) + d\widetilde{S}_\infty(\psi, z;\zeta) = u_\infty - \widetilde{S}_\infty(\psi, z) \tag{3.15}$$

for (η, γ, ζ) and update (ψ, λ, z) into $(\psi + \eta, \mu + \gamma, z + \zeta)$.

These equations contain Fréchet derivatives with respect to z acting as linear operators on ζ. These are obtained by differentiating the kernels with respect to z and are given by

$$d\widetilde{S}(\psi, z;\zeta)(t) = \int_0^{2\pi} dL(t,\tau;z,\zeta)\psi(\tau)\,d\tau, \quad t\in[0,2\pi],$$

where

$$dL(t,\tau;z,\zeta) := -\frac{ik}{2}\,\frac{\{z(t)-z(\tau)\}\cdot\{\zeta(t)-\zeta(\tau)\}}{|z(t)-z(\tau)|}\,H_1^{(1)}(k|z(t)-z(\tau)|)$$

and

$$d\widetilde{K}'(\psi, z;\zeta)(t) = \int_0^{2\pi} dM(t,\tau;z,\zeta)\psi(\tau)\,d\tau, \quad t\in[0,2\pi],$$

where

$$dM(t,\tau;z,\zeta) := \frac{ik}{2}\,\frac{[z'(t)]^\perp\cdot\{z(\tau)-z(t)\}\,\{z(t)-z(\tau)\}\cdot\{\zeta(t)-\zeta(\tau)\}}{|z(t)-z(\tau)|^3}$$
$$\times\left\{k\,|z(t)-z(\tau)|\,H_0^{(1)}(k|z(t)-z(\tau)|) - 2H_1^{(1)}(k|z(t)-z(\tau)|)\right\}$$
$$+\frac{ik}{2}\,\frac{[\zeta'(t)]^\perp\cdot\{z(\tau)-z(t)\}+[z'(t)]^\perp\cdot\{\zeta(\tau)-\zeta(t)\}}{|z(t)-z(\tau)|}\,H_1^{(1)}(k|z(t)-z(\tau)|).$$

Here, we used the relation

$$H_1^{(1)'}(w) = H_0^{(1)}(w) - \frac{1}{w}\,H_1^{(1)}(w).$$

The Fréchet derivative of the far field operator $\widetilde{S}_\infty$ is given by

$$d\widetilde{S}_\infty'(\psi,z;\zeta)(\widehat{x}) = \frac{e^{-i\pi/4}\sqrt{k}}{\sqrt{8\pi}}\int_0^{2\pi} e^{-ik\,\widehat{x}\cdot z(\tau)}\,\widehat{x}\cdot\zeta(\tau)\,\psi(\tau)\,d\tau,\quad \widehat{x}\in\mathbb{S}^1.$$

Finally, for the plane wave incidence $u^i(x)=e^{ik\,x\cdot d}$, we have

$$g(z,\mu)(t) = 2ik\left([z'(t)]^\perp\cdot d+\mu\right)e^{ik\,z(t)\cdot d},$$

and consequently,

$$\partial_z g(z,\mu;\zeta)(t) = 2ik\big\{[\zeta'(t)]^\perp\cdot d + ik([z'(t)]^\perp\cdot d+\mu)\zeta(t)\cdot d\big\}e^{ik\,z(t)\cdot d}.$$

Here, we would like to emphasize the fact that we have explicit representations of the Fréchet derivatives as weakly singular boundary integral operators which allow for a straightforward discretization as opposed to the discretization of the Fréchet derivatives of the forward operator $\mathcal{F}$ based on the characterization (1.6).

Now, for finitely many incident fields $u_1^i,\dots,u_M^i$ and corresponding far field patterns $u_{\infty,1},\dots,u_{\infty,M}$, summarizing, we describe one iteration step of our algorithm as follows: given an approximation z for the parameterization of the boundary ∂D and $\mu = |z'|\,\lambda\circ z$ for the impedance function on ∂D and $\psi_1,\dots,\psi_m$ for the densities, after abbreviating

$$g_m(z,\mu) := 2[z']^\perp\cdot \mathrm{grad}u_m^i\circ z + 2ik\mu u_m^i\circ z, \tag{3.16}$$

we solve the linearized system

$$\begin{aligned}&\eta_m-\widetilde{K}'(\eta_m,z)-ik\mu\widetilde{S}(\eta_m,z)-ik\gamma\widetilde{S}(\psi_m,z)-2ik\gamma u_m^i\circ z\\ &\quad -d\widetilde{K}'(\psi_m,z;\zeta)-ik\mu d\widetilde{S}(\psi_m,z;\zeta)-dg_m(z;\zeta)\\ &\quad = g_m(z,\mu)-\psi_m+\widetilde{K}'(\psi_m,z)+ik\mu\widetilde{S}(\psi_m,z)\end{aligned} \tag{3.17}$$

and

$$\widetilde{S}_\infty(\eta_m,z)+d\widetilde{S}_\infty(\psi_m,z;\zeta)=u_\infty-\widetilde{S}_\infty(\psi_m,z), \tag{3.18}$$

where $m = 1,\dots,M$. We solve the system (3.17)–(3.18) of $2M$ equations for the $2+M$ unknowns ζ, γ and η_m, $m=1,\dots,M$, and update z into $z+\zeta$, μ into $\mu+\gamma$ and ψ_m into $\psi_m+\eta_m$.

For the initial step of the iteration, only an initial guess for the shape z and the impedance $\mu=|z'|\,\lambda\circ z$ is required. The initial densities ψ_m can then be obtained by solving the parametrized equation (3.6), that is, (3.10).

Due to the ill-posedness, stabilization, for example, by Tikhonov regularization is required in each iteration step. For this, we suggest an L^2 penalization for the densities and an H^p Sobolev penalty term for some small $p\in\mathbb{N}$ for the boundary parameterization and the impedance function.

4. Connection with the forward operator. We can relate the above approach to the Newton iterations from [**7**] for solving the inverse obstacle scattering problem previously mentioned in the introduction. Denoting by $F:(z,\mu)\to u_\infty$, the operator that maps the boundary ∂D represented by the parameterization z and the impedance function $\mu=|z'|\,\lambda\circ z$ onto the far field pattern for scattering of the incident wave u^i from the impedance obstacle D, the inverse problem is equivalent to solving the nonlinear operator equation

$$F(z,\mu)=u_\infty. \tag{4.1}$$

Linearization leads to

$$\partial_z F(z,\mu;\zeta)+\partial_\mu F(z,\mu;\gamma)=u_\infty-F(z,\mu), \tag{4.2}$$

which must be solved for ζ and γ in order to update an approximation z and μ into $z+\zeta$ and $\mu+\gamma$.

If we assume that k^2 is not a Dirichlet eigenvalue for the negative Laplacian, as noted in connection with Theorem 3.1, in view of the system (3.10)–(3.11), we can express the forward map in the form

$$F(z,\mu) = \widetilde{S}_\infty(A(z,\mu)g(z,\mu), z) \tag{4.3}$$

with g defined by (3.13). Here, we have abbreviated

$$A(z,\mu) := \left(I - \widetilde{K}'(\cdot,z) - ik\mu\widetilde{S}(\cdot,z)\right)^{-1}.$$

By the product and chain rule this implies the total Fréchet derivative

$$\begin{aligned}\partial_z F(z,\mu;\zeta) + \partial_\mu F(z,\mu;\gamma) &= d\widetilde{S}_\infty\,(A(z,\mu)g(z,\mu), z;\zeta)\\ &+ \widetilde{S}_\infty(A(z,\mu)[d\widetilde{K}' + ik\mu d\widetilde{S}](A(z,\mu)g(z,\mu), z;\zeta), z)\\ &+ ik\widetilde{S}_\infty(A(z,\mu)\gamma\widetilde{S}(A(z,\mu)g(z,\mu), z)\\ &+ \widetilde{S}_\infty(A(z,\mu)(dg(z,\mu;\zeta) + ik\gamma u^i\circ z), z).\end{aligned} \tag{4.4}$$

Now, we can establish the following interrelation between our proposed iterative scheme and the Newton iterations for the forward map F.

Theorem 4.1. *Assume that k^2 is not a Dirichlet eigenvalue of the negative Laplacian in D, and set*

$$\psi := A(z,\mu)g(z,\mu).$$

Provided ζ and γ satisfy the linearized forward equation (4.2)*, then*

$$\begin{aligned}\eta := A(z,\mu)[d\widetilde{K}'(\psi,z;\zeta) + ik\mu d\widetilde{S}(\psi,z;\zeta)\\ + ik\gamma\widetilde{S}(\psi,z) + dg(z,\mu;\zeta) + ik\gamma u^i\circ z]\end{aligned}$$

and ζ and γ satisfy the linearized equations (3.14) *and* (3.15)*. Conversely, if η, ζ and γ solve* (3.14) *and* (3.15)*, then ζ and γ satisfy* (4.2)*.*

Proof. From (4.2), (4.3) and the definition of ψ, we have

$$\partial_z F(z,\mu;\zeta) + \partial_\mu F(z,\mu;\gamma) = u_\infty - \widetilde{S}_\infty(\psi,z).$$

The representation (4.4) of the derivative of F yields

$$\partial_z F(z,\mu;\zeta) + \partial_\mu F(z,\mu;\gamma) = d\widetilde{S}_\infty(\psi,z;\zeta) + \widetilde{S}_\infty(\eta,z)$$

and, combining this with the previous equation establishes that (3.15) holds. From the definition of η we observe that (3.14) is also satisfied since its right hand side vanishes for $\psi = A(z,\mu)g(z,\mu)$.

Conversely, (3.14) implies that

$$\eta = A(z,\lambda)\chi,$$

where

$$\begin{aligned}\chi := ik\gamma\widetilde{S}(\psi, z) + 2ik\gamma u^i \circ z + d\widetilde{K}'(\psi, z; \zeta)\\ + ik\mu d\widetilde{S}(\psi, z; \zeta) + \partial_z g(z, \mu; \zeta)\end{aligned}$$

since, as already observed, the right hand side of (3.14) vanishes due to the choice of ψ. Inserting this into (3.15) leads to

$$d\widetilde{S}_\infty(\psi, z, \zeta) + \widetilde{S}_\infty A(z,\lambda)\chi = u_\infty - \widetilde{S}_\infty(\psi, z)$$

and, via (4.3) and (4.4), this implies (4.2). □

Based on Theorem 4.1, the result from **[7]** on injectivity of the derivative of F can be carried over to the present case by the next corollary.

Corollary 4.2. *With the restriction to real valued impedance functions, at the exact solution, the system* (3.10)–(3.11) *is injective, provided* $\lambda \geq 1$.

Indeed, if λ is real valued, the two complex valued equations (3.10) and (3.10) formally determine the complex valued density ψ and the two real valued functions z and $\mu = \lambda \circ z$. In one of our numerical examples we will provide reconstructions using only one incident wave.

Theorem 3.1 also illustrates the difference between the iteration based on the simultaneous linearization of the two integral equations (3.10) and (3.11) and the Newton iterations for (4.1). In general, when placing (3.14) and (3.15) in the sequence of updates, the relation $\psi = A(z,\mu)g(z,\mu)$ between the current approximations for the shape and the impedance z and μ, as well as for the density ψ, will not be satisfied. (This condition will hold for only the first step.) This observation also indicates a possibility for using (3.10) and (3.11) to implement the Newton scheme for (4.1). We merely need to change the update $\psi + \eta$ for the density into $A(z,\mu)g(z,\mu)$ at the expense of throwing away η and solving (3.6) with the updated z and μ for a new density. As opposed to this possibility, we pointed out in the introduction that, in [**7**], the implementation of Newton iterations for (4.1) is based upon the characterization of the Fréchet derivative of F given by (1.6).

5. Numerical implementation. For the numerical implementation, we need to discretize the boundary integral operators S and K' and their Fréchet derivatives. All four operators have kernels of the form

$$K(t,\tau) = K_1(t,\tau)\ln\left(4\sin^2\frac{t-\tau}{2}\right) + K_2(t,\tau) \tag{5.1}$$

with smooth functions K_1 and K_2 and, for their numerical approximation by weighted trigonometric interpolation quadrature, we refer to [**3**]. The factors L_1, M_1, dL_1 and dM_1 in the decomposition of the kernel function L, M, dL and dM corresponding to (5.1) are obtained by replacing the Hankel function in the definitions of L, M, dL and dM by the corresponding Bessel function multiplied by a factor of i/π. For the convenience of the reader, we provide the diagonal elements of the smooth parts as

$$L_1(t,t) = M_1(t,t) = dL_1(t,t) = dM_1(t,t) = 0$$

and, with the Euler-Mascheroni constant

$$C = \lim_{n\to\infty}\left(\sum_1^n (1/k) - \ln(n)\right),$$

$$L_2(t,t) = \frac{i}{2} - \frac{C}{\pi} - \frac{1}{\pi}\ln\left(\frac{k}{2}|z'(t)|\right),$$

$$M_2(t,t) = -\frac{1}{2\pi}\frac{[z'(t)]^\perp\cdot z''(t)}{|z_1'(t)|^2}, \qquad dL_2(t,t) = -\frac{z'(t)\cdot\zeta'(t)}{\pi\,|z'(t)|^2},$$

$$dM_2(t,t) = \frac{|z'(t)|^2\left\{[z'(t)]^\perp\cdot\zeta''(t) + [\zeta'(t)]^\perp\cdot z''(t)\right\}}{2\pi\,|z'(t)|^4} - \frac{2[z'(t)]^\perp\cdot z''(t) z'(t)\cdot\zeta'(t)}{2\pi\,|z'(t)|^4}.$$

When solving the system (3.10)–(3.11), in principle, the parameterization of the update is not unique. To cope with this ambiguity, one possibility that we pursued in our numerical examples was to allow only parameterizations of the form

$$z(t) = r(t)(\cos t, \sin t), \quad 0 \leq t \leq 2\pi, \tag{5.2}$$

with a non-negative function r representing the radial distance of ∂D from the origin. Consequently, the perturbations are of the form

$$\zeta(t) = q(t)(\cos t, \sin t), \quad 0 \leq t \leq 2\pi, \tag{5.3}$$

with a real function q. In the approximations, we assume r and its update q to have the form of a trigonometric polynomial of degree J_z, in particular,

$$q(t) = \sum_{j=0}^{J_z} a_j \cos jt + \sum_{j=1}^{J_z} b_j \sin jt \tag{5.4}$$

with real coefficients a_j and b_j.

We also approximate the unknown (parameterized) impedance function μ by a trigonometric polynomial of degree J_μ and confine ourselves to the case of a real valued impedance function. Then, we collocate the two equations (3.10) and (3.11), each at $2n$ equidistant collocation points, the first equation at the points $t_j = j\pi/n$, $j = 1, \dots, 2n$, and the second equation at the points $(\cos t_j, \sin t_j) \in \mathbb{S}^1$. The resulting linear system for the $2J_z + 2J_\mu + 2$ Fourier coefficients and the $2n$ (or $2nM$ if we use M incident waves) nodal values of the density function ψ is solved in the least squares sense, penalized via Tikhonov regularization. As experienced in the application of regularized Newton iterations for related problems, it is advantageous to use an H^p Sobolev penalty term for the shape and the impedance rather than an L^2 penalty in the Tikhonov regularization for some small $p \in \mathbb{N}$. For the density function, merely L^2 regularization suffices.

The following two numerical examples are intended as proof of the concept and not as indications of an already fully developed method. In particular, the regularization parameters and the number of iterations were chosen by trial and error instead of, for example, a discrepancy principle. In order to avoid committing an inverse crime, the synthetic far field data were obtained by solving the integral equation based on a combined single- and double-layer approach, whereas the inverse solver is based on the single-layer approach.

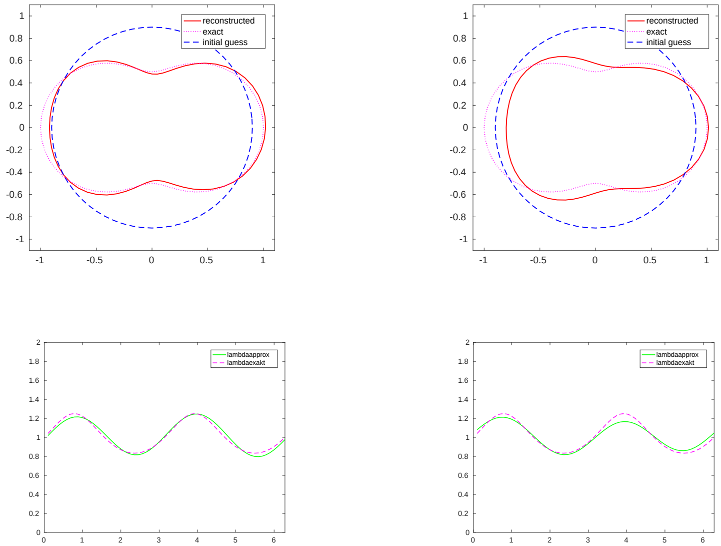

FIGURE 1. Reconstruction of shape (upper) and impedance (lower) of the peanut (5.5) for exact data (left) and 3 percent noise (right).

As boundary curves, we considered a peanut-shaped obstacle with parametric representation

$$z(t) = \sqrt{\cos^2 t + 0.25 \sin^2 t}\,(\cos t, \sin t), \quad 0 \le t \le 2\pi, \tag{5.5}$$

and an apple-shaped obstacle with parametric representation

$$z(t) = \frac{0.5 + 0.4 \cos t + 0.1 \sin 2t}{1 + 0.7 \cos t}\,(\cos t, \sin t), \quad 0 \le t \le 2\pi, \tag{5.6}$$

For both examples, the impedance function was given by

$$\mu(t) = \frac{1}{1 - 0.2 \sin 2t}, \quad t \in [0, 2\pi]. \tag{5.7}$$

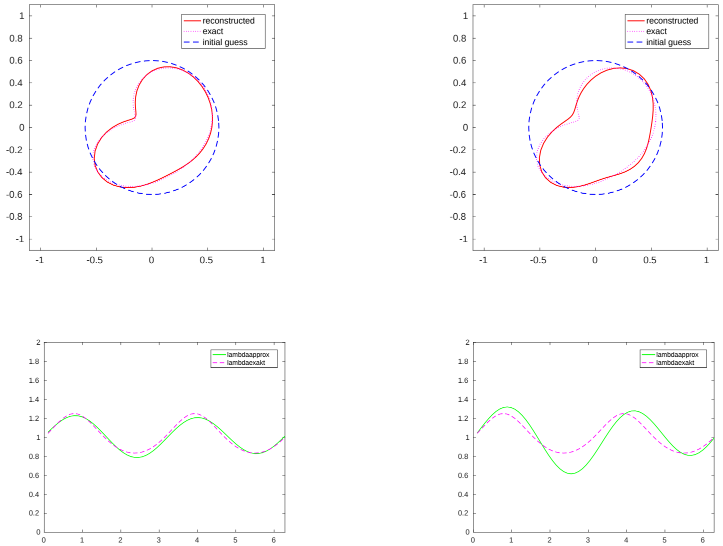

FIGURE 2. Reconstruction of shape (upper) and impedance (lower) of the apple (5.6) for exact data (left) and 3 percent noise (right).

The number of quadrature points was $2n = 64$, both on the boundary curve and on the unit circle for the far field pattern. The wave number was $k = 1$ for the peanut and $k = 3$ for the apple. The degree of the trigonometric polynomials was chosen as $J_z = 4$ and $J_\mu = 2$, and the regularization parameter for an H^2 regularization of both the shape and impedance was 0.001×0.9^m for the mth iteration step for exact data and 0.01×0.9^m for perturbed data. The regularization parameter for the density was 10^{-10} for exact data and 10^{-7} for perturbed data. The iteration was stopped after 20 iterations for exact data and 12 iterations for perturbed data. For the perturbed data, random noise was added point wise with relative error in the L^2 norm. The iterations were begun with an initial guess given by a circle (of radius 0.9 for the peanut and 0.9 for the apple), centered at the origin. For the peanut, we used one incident wave with $d = (1, 0)$ and, for the apple, two incident waves with $d = (\pm 1, 0)$. For the apple, the reconstruction with only one wave also worked but was less accurate.

In the figures, the exact ∂D is given as dotted (magenta), the reconstruction as full (red) and the initial guess as dashed (blue) curve. The exact impedance is given as dotted (magenta) curve and the reconstruction as full (green) curve. In conclusion, we can state that both examples show satisfactory reconstruction and stability.

In closing, we would like to note that, when using more than one incident wave instead of changing the incident direction and keeping the wave number, in principle, we also can use incident waves with one direction and various wave numbers.

Acknowledgments. This research was initiated while the second author was visiting the University of Göttingen. The hospitality and the support by the Research Training Group 2088, *Discovering structure in complex data*: *Statistics meets Optimization and Inverse Problems* are gratefully acknowledged.

REFERENCES

1. F. Cakoni, Y. Hu and R. Kress, *Simultaneous reconstruction of shape and generalized impedance functions in electrostatic imaging*, Inv. Prob. **30** (2014), 105009.

2. F. Cakoni, R. Kress and C. Schuft, *Simultaneous reconstruction of shape and impedance in corrosion detection*, Meth. Appl. Anal. **17** (2010), 357–378.

3. D. Colton and R. Kress, *Inverse acoustic and electromagnetic scattering theory*, Springer, New York, 2012.

4. F. Hettlich, 1995 *Fréchet derivatives in inverse obstacle scattering*, Inv. Prob. **11** (1995), 371–382; *Erratum*, Inv. Prob. **11**, 209–210 (1995).

5. O. Ivanyshyn, R. Kress and P. Serranho, *Huygens' principle and iterative methods in inverse obstacle scattering*, Adv. Comp. Math. **33** (2010), 413-429.

6. R. Kress, *Linear integral equations*, Springer, New York, 2013.

7. R. Kress and W. Rundell, *Inverse scattering for shape and impedance*, Inv. Prob. **17** (2001), 1075–1085.

8. ______, *Nonlinear integral equations and the iterative solution for an inverse boundary value problem*, Inv. Prob. **21** (2005), 1207–1223.

9. J. Liu, G. Nakamura and M. Sini, *Reconstruction of the shape and surface impedance from acoustic scattering data for an arbitrary cylinder*, SIAM J. Appl. Math. **67** (2007), 1124–1146.

10. J. Liu and M. Sini, *On the accuracy of the numerical detection of complex obstacles from far field data using the probe method*, SIAM J. Sci. Comp. **31** (2009), 2665–2687.

11. J. Liu and H. Zhao, *On the reconstruction of obstacle using MFS from the far field data*, Inv. Prob. Sci. Engin. **21** (2013), 682–703.

12. G. Nakamura and M. Sini, *Obstacle and boundary determination from scattering data*, SIAM J. Math. Anal. **39** (2007), 819–837.

13. G. Nakamura and W. Wang, *Reconstruction of an impedance cylinder at oblique incidence from the far-field data*, SIAM J. Appl. Math. **75** (2015), 252–274.

14. P. Serranho, *A hybrid method for inverse scattering for shape and impedance*, Inv. Prob. **22** (2006), 663–680.

15. M. Simsek and N. Tezel, *The reconstruction of shape and impedance exploiting space mapping with inverse difference method*, IEEE Trans. Anten. Propag. **60** (2012), 1868–1877.

Universität Göttingen, Institut für Numerische und Angewandte Mathematik, Lotzestr. 16-18, D 37083 Göttingen, Germany
Email address: **kress@math.uni-goettingen.de**

Texas A&M University, Department of Mathematics, College Station, TX 77843
Email address: **rundell@math.tamu.edu**